THE ASTROPHYSICAL JOURNAL, 335:L61–L65, 1988 December 15

PHOTOMETRY AND THE LIGHT CURVE OF THE OPTICAL COUNTERPART OF THE ECLIPSING MILLISECOND PULSAR 1957+20

S. DJORGOVSKI
Palomar Observatory, California Institute of Technology
AND
CHARLES R. EVANS
Theoretical Astrophysics, California Institute of Technology
Received 1988 August 8; accepted 1988 September 16

ABSTRACT

We confirm the discovery of the optical counterpart to the eclipsing millisecond pulsar 1957+20 recently reported by Fruchter, Stinebring, and Taylor and identified earlier by Kulkarni *et al.* and Fruchter and colleagues. A nearly complete light curve derived from 58 CCD images taken in the Gunn r band has been obtained and found to match the 9.17 hr orbital period of the pulsar. As expected, minimum and maximum light correspond to orbital phases 0.25 and 0.75, respectively. The amplitude of the variation is 0.85 mag with apparent magnitudes of Gunn-Thuan $r = 19.36$, or $V \simeq 19.7$, and colors $(g - r) = 0.66$, or $(B-V) \simeq 1.2$, at maximum light, and uncorrected for interstellar extinction. However, the centroid of the previously proposed optical counterpart displays a 9.17 hr periodic wobble with amplitude of $\sim 0''.5$, indicating the presence of a field star separated by $\simeq 1''$. Assuming that minimum light is due entirely to the field star, the pulsar companion would have peak apparent magnitudes of $r = 20.05$, or $V \simeq 20.3$, and colors $(g - r) = 0.45$, or $(B-V) \simeq 1.0$, again not including extinction. If the extinction is assumed to be $A_V = 1$ mag, the corrected color is found to be $(g - r) = 0.11$, or $(B-V) \simeq 0.7$, which corresponds to an effective temperature of 5800 K. Based on modeling the heating of and reradiation from the companion, we obtain a synthetic light curve that matches the observed sharp rise to maximum light and flat, broad minimum. By matching the model to the observed brightness and color of the counterpart it is possible to rule out a high extinction ($A_V \simeq 3$ mag) to the source due to the high luminosity required. For A_V between 1 and 2 mag the inferred stellar radius lies between 0.07 $R_\odot$ and 0.2 $R_\odot$, depending on distance. Assuming the distance 0.9 kpc derived from the radio dispersion measure, and an extinction of $A_V = 1$ mag, we derive an absolute visual magnitude of the pulsar companion of 10.5 and its radius to be $\simeq 0.16\ R_\odot$, close to that of a degenerate hydrogen dwarf.

Subject headings: photometry — planets: general — pulsars — stars: binaries — stars: variable

I. INTRODUCTION

The recently discovered (Fruchter, Stinebring, and Taylor 1988) eclipsing binary, millisecond pulsar PSR 1957+20 may provide crucial evidence of a link between isolated millisecond pulsars, like PSR 1937+21 and those in globular clusters, and short-period low-mass X-ray binaries (LMXB) (Kluzniak *et al.* 1988; Phinney *et al.* 1988; van den Heuvel and van Paradijs 1988). This system also provides for the first time an opportunity to probe *in situ* the characteristics of the relativistic pulsar wind.

A key element to the potential evolutionary connection is the process of ablation of low-mass stellar companions by the pulsar wind emanating from the rapidly rotating neutron star. The power available in the pulsar wind as the neutron star spins down is $\sim 4 \times 10^{35}$ ergs s^{-1}, given the recently measured $\dot{P} \simeq 3 \times 10^{-20}$ s s^{-1} (J. H. Taylor 1988, private communication). This gives for PSR 1957+20 a timing age of $\tau = P/2\dot{P} \simeq 8.5 \times 10^8$ yr, similar to the previously discovered millisecond pulsars (van den Heuvel, van Paradijs, and Taam 1986; Alpar *et al.* 1982; White and Stella 1988; Phinney *et al.* 1988). Knowledge of this power provides a significant constraint on models of the PSR 1957+20 system, since this energy must be shared between mechanical energy in the stellar wind (responsible for the lengthy radio eclipse) being driven from the $\simeq 0.024\ M_\odot$ companion, reradiated emission from the stellar surface, and X-rays and γ-rays from the shocked pulsar wind.

Optical observations can thus serve to determine the fraction of the pulsar's luminosity that is radiated directly, or created secondarily, in forms able to penetrate ($\kappa \lesssim 0.2$ cm^2 g^{-1}) the photosphere and become reradiated. Such information then constrains the maximum energy available to drive the stellar wind. In addition, the radius and surface temperature can be determined. We report here analysis of a set of detailed optical observations used to determine the photometric parameters and the light variation of the previously identified optical counterpart (hereafter star X) of PSR 1957+20 (Kulkarni, Djorgovski, and Fruchter 1988; Fruchter *et al.* 1988*b*; Fruchter *et al.* 1988*a*).

II. CCD PHOTOMETRY

On the nights of UT 1988 June 7, 8, and 9, we obtained a series of CCD images of the PSR 1957+20 field, using the Mount Palomar 60 inch (1.5 m) telescope. The images were obtained using a TI 800 × 800 CCD detector at the Cassegrain focus, configured in 2 × 2 binning mode (yielding 400 × 400 images with the effective pixel size = 0″.492). The seeing full width at half-maximum (FWHM) was in the range 1″.5–2″, and the conditions were photometric throughout the run. A total of 61 images of the field were taken, 58 in Gunn r band and the

remaining three in Gunn g band. The g band images were obtained at the phases close to minimum and maximum light of star X. The exposures were in the range 400–600 s, depending on the seeing, and taken in succession each night, with approximately 1 minute overhead between exposures for readout, etc. These data were taken over a cumulative period of 9 hr providing a nearly complete (about 92%) coverage of the pulsar orbit, with some phase overlap between the different nights. Additional multiple exposures of *gri* standard stars from Kent (1985) were obtained at a range of air masses each night, for the purposes of flux calibration. The data were processed in a standard fashion, and a digital stellar photometry on the CCD frames was performed using the DAOPHOT package (Stetson 1987).

Measurements of the standard stars were used to define the magnitude zero-points, and determine the color transformations between our instrumental and Kent's (1985) *gr* systems. We adopted his atmospheric extinction coefficients for Mount Palomar, as we found them fully consistent with our own measurements. We obtain the following color equations:

$$g = g_{\rm instr} + 0.14(g - r)_{\rm instr} , \quad (1)$$

$$r = r_{\rm instr} + 0.03(g - r)_{\rm instr} - 0.02 . \quad (2)$$

After applying these color equations, the standard star residuals are ~ 0.01 mag, which is sufficient for our purposes. Aperture magnitudes were used to define the secondary photometric standards among the relatively isolated stars in the PSR 1957+20 field, typically 2 to 3 mag brighter than the proposed optical counterpart. These stars are indicated in Figure 1 (Plate L2), and their *gr* magnitudes are given in Table 1.

The light curve of the proposed counterpart (star X) was obtained through a *relative* photometry, using the crowded-field point-spread function fitting routine NSTAR from the DAOPHOT, and the average magnitude of the secondary standards from Table 1 as the photometric baseline. The magnitude residuals and DAOPHOT error estimates indicate that this photometric baseline is stable on a 0.01 mag level or better,

TABLE 1

PHOTOMETRY OF STARS IN THE PSR 1957+20 FIELD

Star	g	r
B	16.80 ± 0.04	16.13 ± 0.03
E	16.71 ± 0.05	16.04 ± 0.02
F	17.70 ± 0.08	16.92 ± 0.03
G	16.87 ± 0.02	16.11 ± 0.03
I	18.20 ± 0.09	17.12 ± 0.03
K	17.93 ± 0.03	17.04 ± 0.03
O	18.01 ± 0.08	17.23 ± 0.02
P	18.21 ± 0.06	17.38 ± 0.03
Q	17.87 ± 0.04	17.15 ± 0.02
R	17.92 ± 0.08	16.79 ± 0.04
T	18.23 ± 0.06	17.47 ± 0.04
U	17.95 ± 0.04	17.22 ± 0.03
V	18.87 ± 0.07	17.91 ± 0.03
Z	18.70 ± 0.17	18.11 ± 0.02
β	18.81 ± 0.06	18.05 ± 0.02
δ	20.10 ± 0.26	18.97 ± 0.04
λ	19.01 ± 0.05	18.06 ± 0.02
μ	19.13 ± 0.08	17.94 ± 0.04
θ	19.16 ± 0.12	18.25 ± 0.05
υ	18.21 ± 0.23	17.92 ± 0.03
ξ	19.46 ± 0.15	18.30 ± 0.05

and thus the measurement errors of the star X magnitudes are the dominant source of uncertainty. Use of a relative photometry bypasses many possible sources of systematic errors. We also monitored several nearby stars of similar brightness (e.g., D and W in Fig. 1) for internal checks and comparisons. The final light curve of star X and two comparison stars is shown in Figure 2. The light variation is exactly as expected from the radio-determined orbital phases, with minimum light occurring at the pulsar eclipse (phase 0.25), and the peak-to-peak amplitude is $\simeq 0.85$ mag (a factor of 2.2) in the Gunn r band. There is also excellent internal consistency in the data from different nights where the phases overlap. We note that there is no indication of flaring or day-to-day variations larger than a few percent. The light curve is slightly asymmetric.

The magnitude and color of star X at maximum light are as follows: $r = 19.36 \pm 0.05$, and $(g - r) = 0.66 \pm 0.1$; and at minimum light: $r = 20.18 \pm 0.05$, and $(g - r) = 0.99 \pm 0.1$. Using the color transformations given by Kent (1985), these correspond to $V \simeq 19.7$ and $(B-V) \simeq 1.2$ (photospheric temperature $T_{\rm eff} \simeq 4300$ K) at maximum light, and $V \simeq 20.7$ and $(B-V) \simeq 1.55$ ($T_{\rm eff} \simeq 3350$ K) at minimum. These quantities are not corrected for interstellar extinction. If we assume the total extinction on the line of sight to be $A_V = 1$ mag, corresponding to $E_{B-V} = 0.31$ mag, $A_r = 0.76$ mag, and $E_{g-r} = 0.34$ mag, the magnitudes are brighter and the colors bluer by these amounts, and the corrected effective temperatures are $T_{\rm eff} \simeq 5250$ K (at maximum light) and $T_{\rm eff} \simeq 4200$ K (minimum light).

However, as Fruchter *et al.* (1988*a*) and Fruchter *et al.* (1988*b*) reported, there is an apparent motion of the centroid of star X between different orbital phases, most likely caused by the presence of a nearby background or foreground star of similar brightness, which was not resolved by either Kulkarni, Djorgovski, and Fruchter (1988) or Fruchter *et al.* (1988*b*), or by us. Using the digital centering from DAOPHOT, we monitored the effective position of star X and the faint comparison stars relative to the mean positions of the photometric baseline stars. The results are shown in Figure 3. The wobble is following the dimming and brightening of star X, and it has a net peak-to-peak amplitude of $\sim 0\farcs5$ in the NE-SW direction (PA $\simeq 35°$). The most straightforward explanation is that star X is indeed a composite of the real counterpart of the PSR 1957+20 system, which we propose to call X_1, which lies SW from an unrelated foreground or background star $\sim 0\farcs8$–$1''$ away, which we propose to call X_0. Their brightness ratios at different orbital phases will have to be determined from future excellent-seeing observations, as our data do not provide sufficient resolution to constrain their separation and relative brightness.

Instead, we will adopt here a working hypothesis that X_1 contributes no light at the minimum, and that the difference in flux between the minimum and maximum of the light curve represents the net flux from X_1 when seen face-on. Of course, this is actually the upper limit on its brightness. If this is the case, the magnitudes and colors of X_1 at maximum light are as follows: $r = 20.05 \pm 0.1$, and $(g - r) = 0.45 \pm 0.15$, corresponding to $V \simeq 20.3$ and $(B-V) \simeq 1.0$ ($T_{\rm eff} \simeq 4550$ K), not corrected for interstellar extinction. If we assume the interstellar extinction to be $A_V = 1$ mag, as above, the corresponding magnitudes and colors become $r \simeq 19.3 \pm 0.1$, $(g - r) = 0.11 \pm 0.15$, $V \simeq 19.3$, $(B-V) \simeq 0.69$, and $T_{\rm eff} \simeq 5850$ K. [We note that a 0.1 mag error in $(B-V)$ translates to ~ 300 K error in $T_{\rm eff}$ in this range of color and temperature.]

In order to translate the observed magnitudes into physical

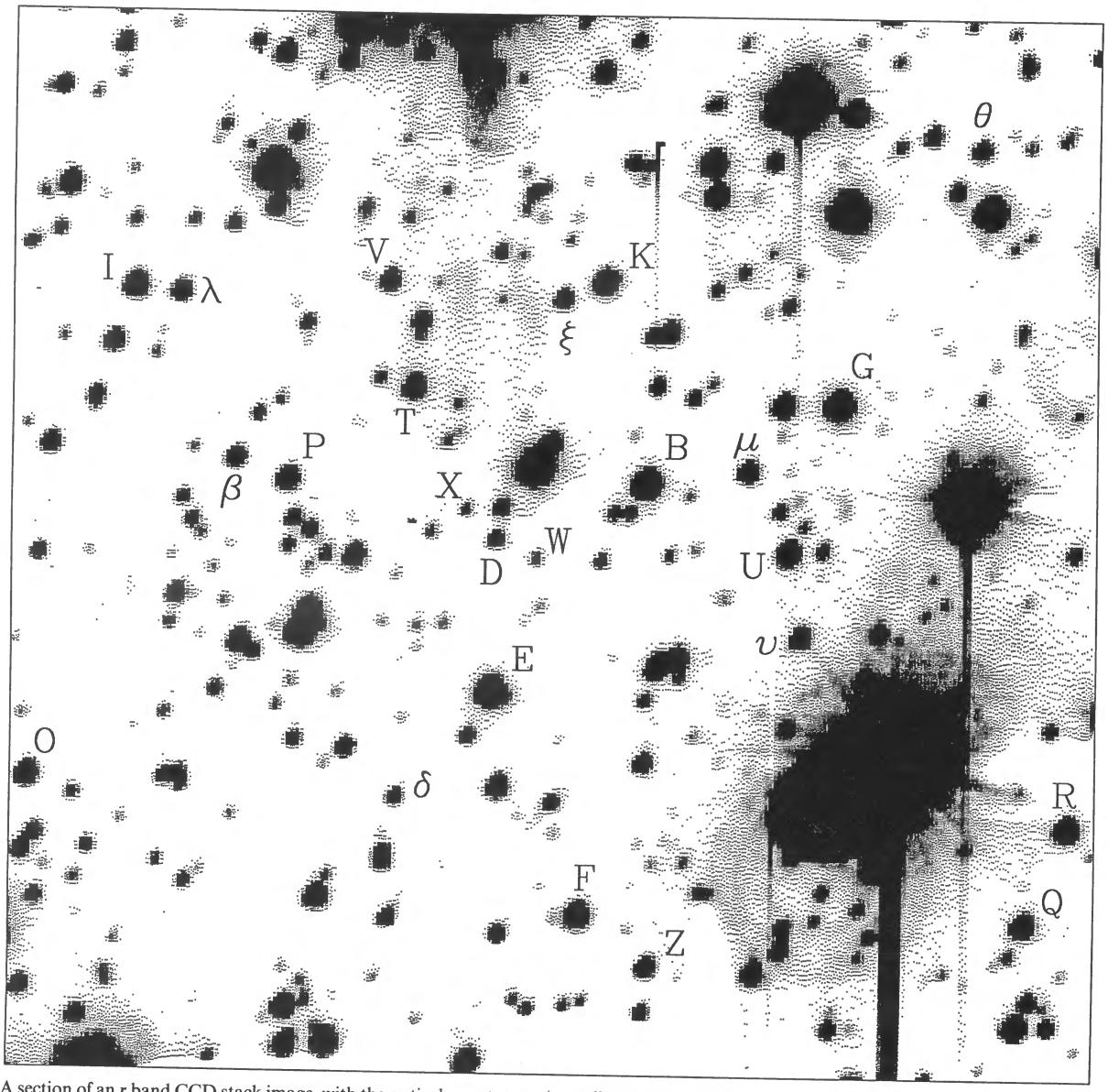

FIG. 1.—A section of an *r* band CCD stack image, with the optical counterpart (actually the SW component of star X), secondary photometric standard stars from Table 1, and the monitoring comparison stars D and W marked. The notation follows and extends that of Kulkarni *et al.* (1988). The field shown is 120″ × 120″, with north to the top and east to the left.

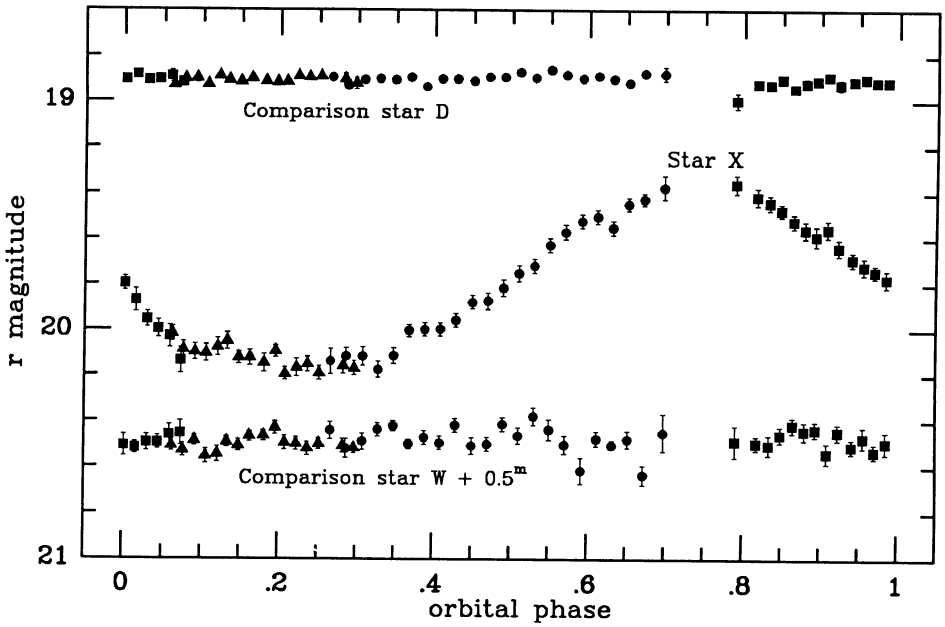

FIG. 2.—The r band light curve of star X as a function of the orbital phase, with the data points from successive nights folded using the pulsar orbital period of 9.17 hr. Different symbols correspond to different nights: *squares*, UT 1988 June 7; *circles*, June 8; and *triangles*, June 9. A peak-to-peak amplitude of ~ 0.85 mag is evident. Maximum and minimum light correlate as expected with the radio-derived phases of opposition and pulsar eclipse, respectively. Error bars are 1 σ. A substantial asymmetry is apparent in the light curve. Also plotted are the corresponding measurements for two comparison stars of similar brightness as star X in its minimum and maximum states.

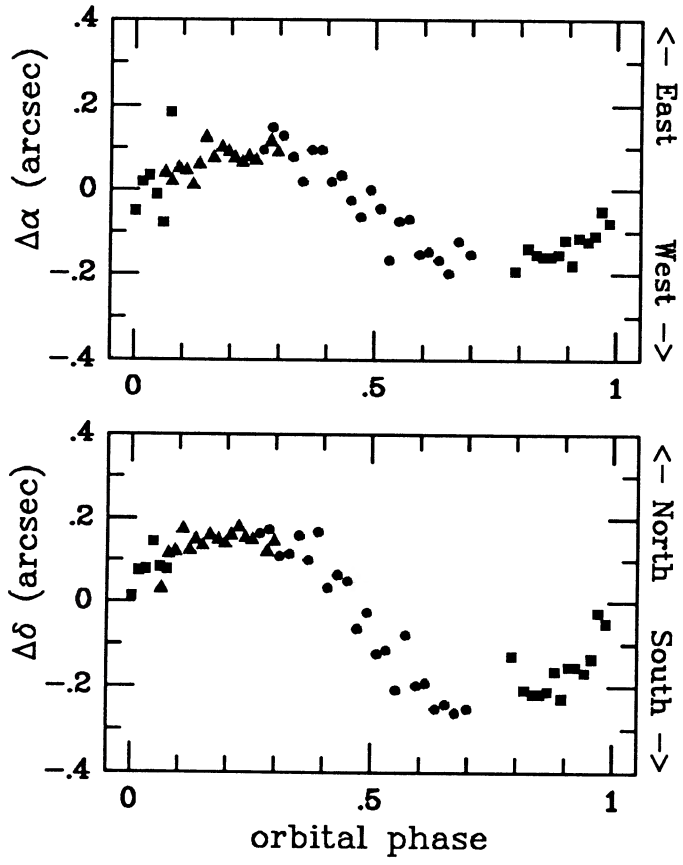

flux units, we used the measurements of Oke-Gunn flux standards (Gunn and Oke 1983) and the Hayes-Latham Vega calibration (Hayes and Latham 1975). Adopting $r_{\rm VEGA} = 0.405$, we estimate that $r = 20$ mag corresponds to 42 μJy at an effective wavelength of 660 nm. In the V band, according to the Hayes-Latham calibration, $V = 20$ mag corresponds to 35 μJy at an effective wavelength of 556 nm. The light curve of star X in linear flux units is shown in Figure 4.

III. LIGHT CURVE SYNTHESIS AND COMPANION RADIUS

The emission and variability of the optical counterpart is almost certainly due to heating from the pulsar. We expect that the relativistic pulsar wind is deflected by a shock lying just above a contact discontinuity separating the pulsar wind from the stellar wind (Phinney *et al.* 1988). This shock should accelerate electrons and positrons to high energies (~ 1 TeV), which subsequently cool in the ~ 30 G magnetic field. Synchrotron-emitted and inverse-Compton–scattered X-rays and γ-rays will result. While soft X-rays may be efficient at heating a corona above the companion and driving off a wind, more energetic γ-rays will be absorbed below the photosphere and produce reradiation at optical wavelengths. The pulsar wind may also contain a relativistic heavy ion (cosmic-ray) component, which would penetrate directly to below the photosphere.

In order to model the light curve, it is necessary to make some assumption about how this incident energy flux is dis-

FIG. 3.—Positional variation of the measured centroids of star X, relative to the baseline defined by the photometric baseline stars. The point-to-point scatter is indicative of the measurement errors. The meaning of the different symbols is as in Fig. 2. The systematic variation of position of star X with orbital phase is direct evidence of its composite nature, an overlap of the optical counterpart of the PSR 1957+20 system with an unresolved background star $\sim 0\farcs8$–$1''$ away to northeast (PA $\simeq 35°$).

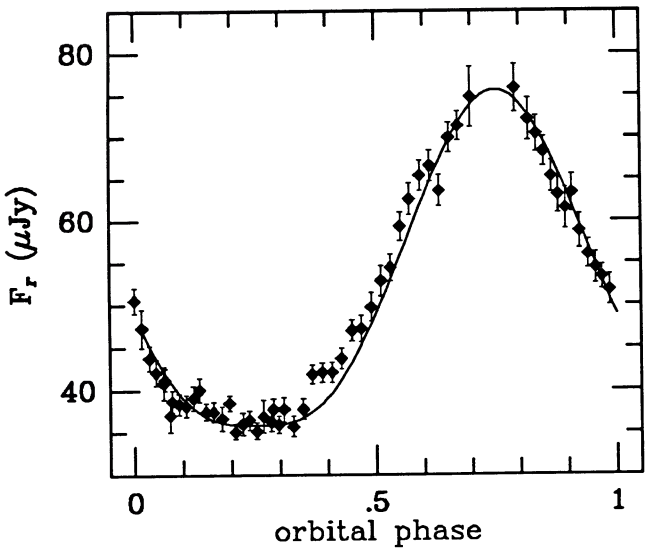

FIG. 4.—The linear flux light curve of star X. The absolute flux in Gunn r band (assuming the conversion that $r = 20$ mag corresponds to 42 μJy) is shown vs. orbital phase, with points from successive nights folded using the pulsar orbital period of 9.17 hr. The intensity at minimum light may be due mostly or entirely to the unresolved background star. The asymmetry apparent in the light curve is probably evidence of distortion of the pulsar wind shock and contact discontinuity above the low-mass companion due to Coriolis acceleration. The solid line represents our model light curve, which is more fully described in the text.

tributed over the stellar surface. The simplest assumption is to initially ignore the presumed intervening pulsar wind shock and imagine direct illumination of the companion from the pulsar. If the radiation flux in forms capable of penetrating the photosphere is $f_{\rm phot} < f_{\rm psr}$, then the absorbed flux on the surface is $F = f_{\rm phot} \cos \zeta$, where ζ is the angle of foreshortening. The local effective temperature is then a function of position $T_{\rm eff} = (f_{\rm phot} \cos \zeta/\sigma)^{1/4}$, which would provide a major contribution to the optical variation with orbital phase.

The intensity and spectrum of the radiation emerging from the surface is a function of emitted direction (limb darkening). While a correct treatment would require a detailed knowledge of the stellar atmosphere of the companion, the overall energetics should be reasonably well modeled by the Eddington approximation. This relates the matter temperature $T^4 = (1/2)T_{\rm eff}{}^4[1 + (3/2)\tau]$ to the (vertical) optical depth. We can then approximate the emergent intensity $I_\nu(0, \mu)$ into a direction having $\mu = \cos \vartheta$ to be given by the Planck function of the temperature at a line-of-sight optical depth of unity: $I_\nu(0, \mu) = B_\nu(T_*)$, where $T_*{}^4 = (1/2)T_{\rm eff}{}^4[1 + (3/2)\mu]$. This displays the approximate limb-darkening dependence. The net apparent flux in any direction, given by ϑ, is modeled by integrating over the visible surface and over a given photometric band b_i

$$F_{b_i} = \frac{15}{2\pi^5}\left(\frac{R}{D}\right)^2 \int d\theta\, d\phi \sin\theta F(\theta, \phi; \cos\zeta) \times \cos\vartheta\left(1 + \frac{3}{2}\cos\vartheta\right) \int_{b_i} \frac{x^3\, dx}{e^x - 1}, \quad (3)$$

where D is the distance to the system, R is the companion's radius, and $x = h\nu/kT_*$ is the dimensionless frequency.

We first use our measurements of apparent visual magnitude and color to fix (subject to extinction and unknown distance)

TABLE 2

PHYSICAL PARAMETERS OF THE PSR 1957+20 COMPANION (STAR X_1)

A_V (mag)	D (kpc)	R (cm)	$L_{\rm opt}$ (ergs s^{-1})	$L_{\rm tot}$ (ergs s^{-1})
0.....	0.4	6.5×10^9	4.2×10^{30}	$>1.3 \times 10^{34}$
	0.9	1.5×10^{10}	2.1×10^{31}	$>1.3 \times 10^{34}$
1.....	0.4	5.3×10^9	7.8×10^{30}	$>3.6 \times 10^{34}$
	0.9	1.2×10^{10}	4.0×10^{31}	$>3.6 \times 10^{34}$
	2.0	2.7×10^{10}	2.0×10^{32}	$>3.6 \times 10^{34}$
	0.9	8.3×10^9	1.1×10^{32}	$>2.1 \times 10^{35}$
	2.0	1.9×10^{10}	5.4×10^{32}	$>2.1 \times 10^{35}$
3.....	0.9	5.6×10^9	8.0×10^{32}	$>3.3 \times 10^{36}$
	2.0	1.3×10^{10}	3.9×10^{33}	$>3.3 \times 10^{36}$

the stellar radius R. Using the Hayes-Latham (1975) calibration, we find the integrated flux (ergs cm^{-2} s^{-1}) in the V band is given by $V - A_V = -2.5 \log F_V - 13.8$. For apparent magnitude $V = 20.3$, with no extinction, this is $F_V = 2.29 \times 10^{-14}$ ergs cm^{-2} s^{-1}. With extinction, the flux is appropriately higher. The reddening corrected color is $(B - V) = 2.5 \log (F_V/F_B) + 0.913$. By calculating the flux integrals (3) for both V and B bands, when the companion is at opposition, the ratio of fluxes can be used with the color to determine the heating flux $f_{\rm phot}$. Once the incident flux is known, the returned flux in the V band can be determined and compared to the observed F_V. If the distance to PSR 1957+20 were known, this determines the radius R of the companion.

We have calculated a set of models based on different assumed values of extinction. The implied radii are given for a set of these models in Table 2. Figure 5 summarizes the dependence of inferred stellar radius on distance and extinction. Once the extinction is known and a better determination of the distance is available (perhaps from the pulsar timing), it will be

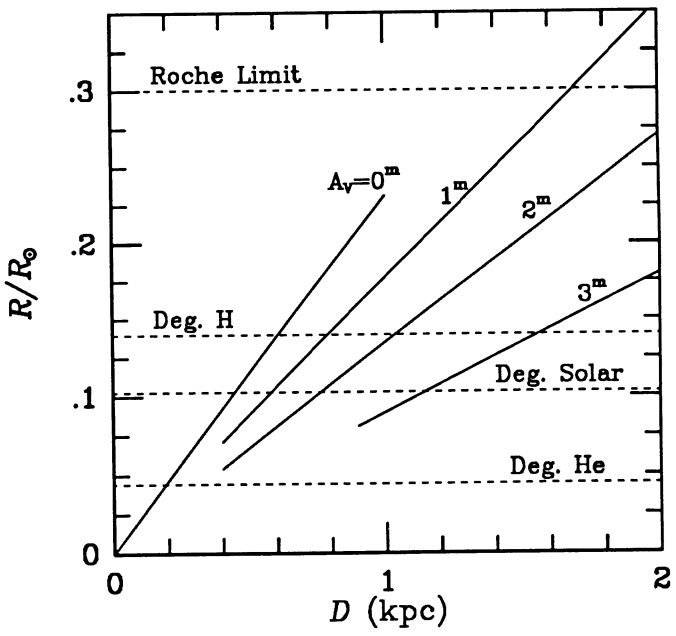

FIG. 5.—Constraints on the stellar radius of the low mass companion in the PSR 1957+20 system. Solutions are shown dependent on the unknown distance and extinction. For comparison the radii of degenerate helium, solar composition, and hydrogen stars are shown, as well as the Roche radius of the companion. The range of likely radii is discussed further in the text.

possible to fix the radius of the low-mass companion. Our modeling determines an approximate relationship for the radius (in cm):

$$\log R = \log D_{\rm kpc} - 0.126 A_V + 10.21 \ . \quad (4)$$

The total reradiated optical luminosity can be calculated from these models as well, and values are given in Table 2. On the assumption that the pulsar wind (and hence $L_{\rm psr}$) is isotropic, a lower limit on the *total* pulsar luminosity can be obtained. The limit on $L_{\rm psr}$ is only a function of extinction and values are given in Table 2. We see that $A_V = 3$ requires $L_{\rm psr} > 3.3 \times 10^{36}$ ergs s^{-1}, which implies a timing age of $\tau < 9 \times 10^7$ yr. With the measured timing age, we believe an extinction as high as $A_V = 3$ to the pulsar is effectively ruled out. Even $A_V = 2$ requires that $>50\%$ of the flux incident on the companion go into optical emission, which is high if energy is to be available to drive the stellar wind and emission also occurs in X-rays and γ-rays.

Hence the extinction probably lies between $A_V = 0$ and $A_V = 2$. If the distance is as low as 0.4 kpc, then the inferred radius is still larger than that of a helium degenerate dwarf and is only close if the extinction is $A_V = 2$ at 0.4 kpc. Unless D is significantly less than 0.4 kpc, a helium degenerate star is likely ruled out. For $D = 0.8$ kpc (close to the dispersion measure derived distance), $A_V = 1$ or $A_V = 2$ would place the radius somewhere between a degenerate pure hydrogen star, $R = 0.14\ R_\odot$, and a degenerate star of solar composition, $R = 0.10\ R_\odot$, as predicted by Phinney *et al.* (1988). For $D = 1.6$ kpc, the same range in A_V would imply nondegenerate, thermally supported radii up to the Roche radius $\simeq 0.3\ R_\odot$, though even for $A_V = 2$ the $T_{\rm eff} \simeq 7000$ K should imply a cooling time scale shorter than the ablation time scale (Phinney *et al.* 1988).

With the heating flux determined, a synthetic light curve can be generated. Equation (3) was calculated in the r band for a series of points at different orbital phases. Figure 4 shows the theoretical light curve superposed on the measured *flux* in Gunn r band. Again, it is assumed that only the field star contributes at minimum light. The effects of limb darkening and foreshortened absorption combine to yield a peaked maximum and flattened minimum. We see that the synthesized light curve fits quite well overall, though no account has been made for the observed asymmetry.

We believe the slight asymmetry in the light curve is evidence for an intervening pulsar wind shock and boundary between the two winds. The Coriolis acceleration on the stellar wind then naturally produces an asymmetric shock and interface. Close examination of the light curve in Figure 4 shows that most of the asymmetry can be accounted for by giving the theoretical light curve a phase *shift* of about -0.01. We can roughly see how this comes about by considering the angular rotation produced in material liberated from the companion's surface before reaching the contact discontinuity at the eclipse radius $R_E \simeq 0.7\ R_\odot$. The Coriolis rotation is approximately $\Omega t_w = \Omega R_E v_w^{-1}$, where Ω is the orbital rotation rate, t_w is the crossing time to the eclipse radius, and v_w is the stellar wind velocity. Using $\Omega = 1.9 \times 10^{-4}$ and taking $v_w \simeq 700$ km s^{-1}, the wind rotates in the retrograde direction by ~ 0.02 in phase. The sign is right, allowing the pulsar shock to present a higher aspect to the pulsar on the trailing side of the companion. This presumably provides a somewhat stronger pulsar wind shock on this side, generating more secondary radiation and giving a more rapid rise to maximum light.

A model for the illumination of the companion [that specifies $F(\theta, \phi)$ in eq. (3)] which takes into account the intervening pulsar wind shock and production of secondary radiation will be difficult to develop. The total optical luminosity and basic characteristics of the light curve are not likely to differ radically. However, as high-resolution images become available to determine the true minimum light of the optical counterpart and more multicolor photometry and spectra are obtained, more sophisticated modeling will be clearly useful.

We thank J. Roth, S. Staples, and the staff at Palomar Observatory for assistance with the observations. We acknowledge stimulating discussions with S. Kulkarni and E. S. Phinney. The Palomar 60 inch telescope is operated jointly by the California Institute of Technology and the Carnegie Institution of Washington. This work was supported in part by NSF grant AST 85-14911 (C. R. E.). S. D. acknowledges partial support from California Institute of Technology.

REFERENCES

Alpar, M. A., Cheng, A. F., Ruderman, M. A., and Shaham, J. 1982, *Nature*, **300**, 728.
Fruchter, A. S., Gunn, J. E., Djorgovski, S., Kulkarni, S. R., and Dressler, A. 1988*a*, *IAU Circ.*, No. 4617.
Fruchter, A. S., Gunn, J. E., Lauer, T. R., and Dressler, A. 1988*b*, *Nature*, **334**, 686.
Fruchter, A. S., Stinebring, D. R., and Taylor, J. H. 1988, *Nature*, **333**, 237.
Gunn, J. E., and Oke, J. B. 1983, *Ap. J.*, **266**, 713.
Hayes, D., and Latham, D. 1975, *Ap. J.*, **197**, 593.
Kent, S. 1985, *Pub. A.S.P.*, **97**, 165.
Kluzniak, W., Ruderman, M., Shaham, J., and Tavani, M. 1988, *Nature*, **334**, 225.
Kulkarni, S. R., Djorgovski, S., and Fruchter, A. S. 1988, *Nature*, **334**, 504.
Phinney, E. S., Evans, C. R., Blandford, R. D., and Kulkarni, S. R. 1988, *Nature*, **333**, 832.
Stetson, P. 1987, *Pub. A.S.P.*, **99**, 191.
van den Heuvel, E. P. J., and van Paradijs, J. 1988, *Nature*, **334**, 227.
van den Heuvel, E. P. J., van Paradijs, J., and Taam, R. E. 1986, *Nature*, **322**, 153.
White, N. E., and Stella, L. 1988, *Nature*, **332**, 416.

Note added in proof.—Our new imaging in subarcsecond seeing from Palomar clearly resolves star X into two components, as proposed here, and in complete agreement with the observations of J. van Paradijs *et al.* (1988, *Nature*, **334**, 684). We thank A. Fruchter for a helpful comment on the pulsar ephemerides.

S. Djorgovski: Palomar Observatory, 105–24, California Institute of Technology, Pasadena, CA 91125

Charles R. Evans: Theoretical Astrophysics, 130–33, California Institute of Technology, Pasadena, CA 91125